Organic & Biomolecular Chemistry

Cite this: *Org. Biomol. Chem.*, 2012, **10**, 4704

www.rsc.org/obc

PAPER

Blue-light-emitting multifunctional triphenylamine-centered starburst quinolines: synthesis, electrochemical and photophysical properties†

Peng Jiang,[a] Dong-Dong Zhao,[a] Xiao-Li Yang,[a] Xiao-Lin Zhu,[a] Jin Chang[b] and Hong-Jun Zhu*[a]

Received 16th January 2012, Accepted 12th April 2012
DOI: 10.1039/c2ob25120e

A series of triphenylamine-centered starburst quinolines (**1a–1g**) have been synthesized by Friedländer condensation of the 4,4′,4″-triacetyltriphenylamine (**2**) and 2-aminophenyl ketones (**3a–3g**) in the presence of catalytic sulfuric acid and characterized well. They are thermally robust with high glass transition temperatures (above 176.4 °C) and decomposition temperatures (above 406 °C). These compounds emit blue fluorescence with λ_{max}^{Em} ranging from 433 to 446 nm in dilute toluene solution and 461 to 502 nm in the solid-state and have a relatively high efficiency (Φ_u = 0.98–0.57). **1a–1g** have estimated ionization potentials (IP) of 4.54 to 6.45 eV which are significantly near or higher than those of well-known electron transport materials (ETMs), including tris(8-hydroxyquinoline)aluminium (Alq_3) (IP = 5.7–5.9 eV), and previously reported oligoquinolines (IP = 5.53–5.81 eV). Quantum chemical calculations using DFT B3LYP/6-31G* showed the highest occupied molecular orbital (HOMO) of −5.05 to −4.81 eV, which is close to the work function of indium tin oxide (ITO). These results demonstrate the potential of **1a–1g** as hole-transporting/light-emitting/electron-transport materials and the host-materials of a dopant for hole-injecting for applications in organic light-emitting devices.

Introduction

Organic light-emitting devices (OLEDs) have attracted a great deal of attention because of their wide applications in high-resolution, full-color, flat-panel displays and solid-state illumination sources, since the first application of a multilayer thin-film structure in OLEDs by Tang *et al.*[1–8] In the past two decades, small molecules and polymers have received the most attention in the field of OLEDs.[9] An important factor for achieving high device efficiency in the field is maintaining a balance between electron and hole currents.[10] Different strategies have been developed to meet the requirement of charge balance, which includes the employment of multilayered structures and the introduction of bipolar or multifunctional molecules like dendrimers or starbursts.[11–21] Meanwhile, triarylamine (TPA) and its derivatives have long been exploited as hole-transport layers (HTLs) for OLEDs, and their range of application is continuously widening.[22–24] Quinoline and its derivatives are also most commonly used as building blocks for increasing electron affinity of current electron transport materials for OLEDs.[25] Thus the combination of the hole-transporting triphenylamine moiety and the electron-transporting quinoline moiety in tris(8-quinoline)-triphenylamine (TQTPA) gives it bipolar charge transport property. Above studies and reports on TQTPA showed that the bipolar starburst molecule, TQTPA exhibited desirable thermal stability, luminescence property and excellent hole-transporting ability.[26]

Moreover, owing to its excellent thermal stabilities from its three-dimensional propeller structure, TPA is a good choice as the central core for starburst molecules. The starburst molecules, tris(4-(quinolin-5-yl)phenyl)amine (TPAQ-1)[27] and 3-(naphthalen-1-yl)-*N*-(3-(naphthalen-1-yl)phenyl)-*N*-(3-(quinolin-8-yl)-phenyl)aniline (TPAQ-2)[28] had been synthesized and used for light-emitting materials in OLEDS, with excellent thermal stability and luminescence properties. However, the reports concerning the electrochemical and photophysical properties of the starbursts based on triphenylamine-centered starburst 4-substituted quinolines are limited. In this context, we aim to develop new triphenylamine-centered starburst 4-substituted quinolines molecules and further study the underlying structure–property relationships.

In this paper, we report the synthesis and investigation of the thermal stabilities, electrochemical and photophysical properties of a series of novel triphenylamine-centered starburst quinolines: tris(4-(4-phenylquinolin-2-yl)phenyl)amine (**1a**), tris(4-(4-(4-bromophenyl)quinolin-2-yl)phenyl)amine (**1b**), tris(4-(4-

[a]*Department of Applied Chemistry, College of Science, Nanjing University of Technology, Jiangsu Key Laboratory of Industrial Water-Conservation & Emission Reduction, Nanjing 210009, China. E-mail: zhuhjnjut@hotmail.com; Fax: +86 25 83587443; Tel: +86 25 83172358*
[b]*Discipline of Chemistry, Queensland University of Technology, 2 George St, Brisbane (QLD), 4000, Australia*

†Electronic supplementary information (ESI) available: Experimental details and characterization data of new compounds **3d**, **3f–3g**, **1a–1g**; mass spectra of **3d**, **3f–3g** and NMR spectra of **3d**, **3f–3g**, **1a–1g**; calculation results of **1a–1g**. See DOI: 10.1039/c2ob25120e

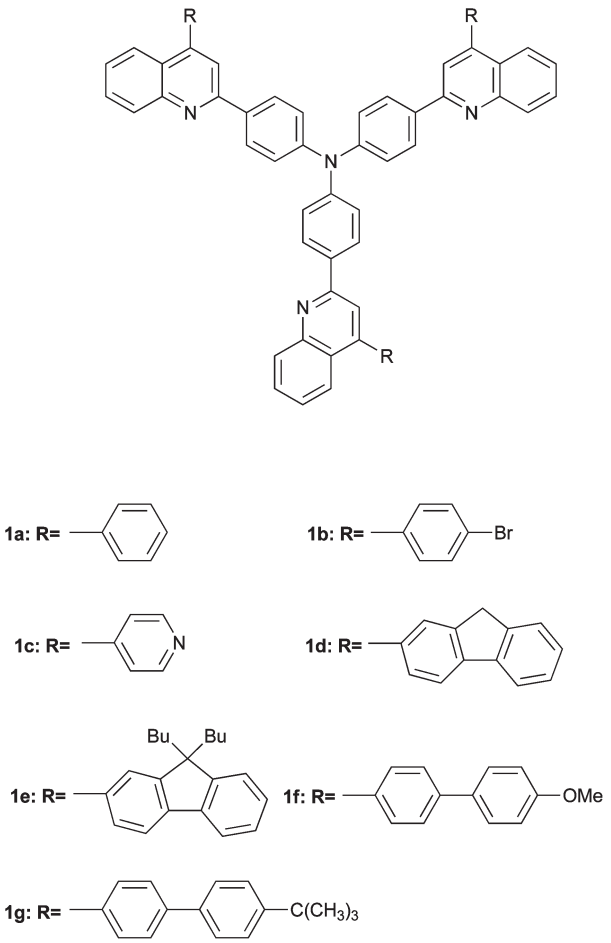

Chart 1 Structures of seven triphenylamine-centered starburst quinolines.

(pyridin-4-yl)quinolin-2-yl)phenyl)amine (**1c**), tris(4-(4-(9*H*-fluoren-2-yl)quinolin-2-yl)phenyl)amine (**1d**), tris(4-(4-(9,9-dibutyl-9*H*-fluoren-2-yl)quinolin-2-yl)phenyl)amine (**1e**), tris(4-(4-(4′-methoxybiphenyl-4-yl)quinolin-2-yl)phenyl)amine (**1f**) and tris(4-(4-(4′-*tert*-butylbiphenyl-4-yl)quinolin-2-yl)phenyl)amine (**1g**) (shown in Chart 1). These starbursts show superior properties including relatively high fluorescence quantum efficiency, excellent thermal stabilities, high ionization potential and highest occupied molecular orbitals (HOMO) proximate to the work function of indium tin oxide (ITO), which make them possible candidates for a class of hole-injecting/hole-transporting/light-emitting/electron-transport material in OLEDs.

Results and discussion

Synthesis

As shown in Scheme 1, all seven new target compounds **1a–1g** were synthesized by a sulfuric acid-catalyzed Friedländer reaction with 4,4′,4″-triacetyltriphenylamine (**2**) and 2-aminophenyl ketones (**3a–3g**) in 41–33% yield, respectively (Scheme 1).[29] The sulfuric acid catalyst and acetic acid as a solvent were readily removed by precipitation into a 25% ammonia solution in water. The materials were passed through silica-gel columns *via* flash chromatography to remove polar byproducts. They were subsequently recrystallized twice in tetrahydrofuran–methanol mixtures ranging from 30 to 50% methanol. The compound **2** was synthesized by acetylation of triphenylamine with acetyl chloride and aluminium trichloride in dichloromethane at reflux temperature (Scheme 2) in high yields 92%.[30] The intermediates **3a–3e** were obtained *via* the Sugasawa reaction, which starts from an aniline and a series of different nitriles **4a–4e** in the

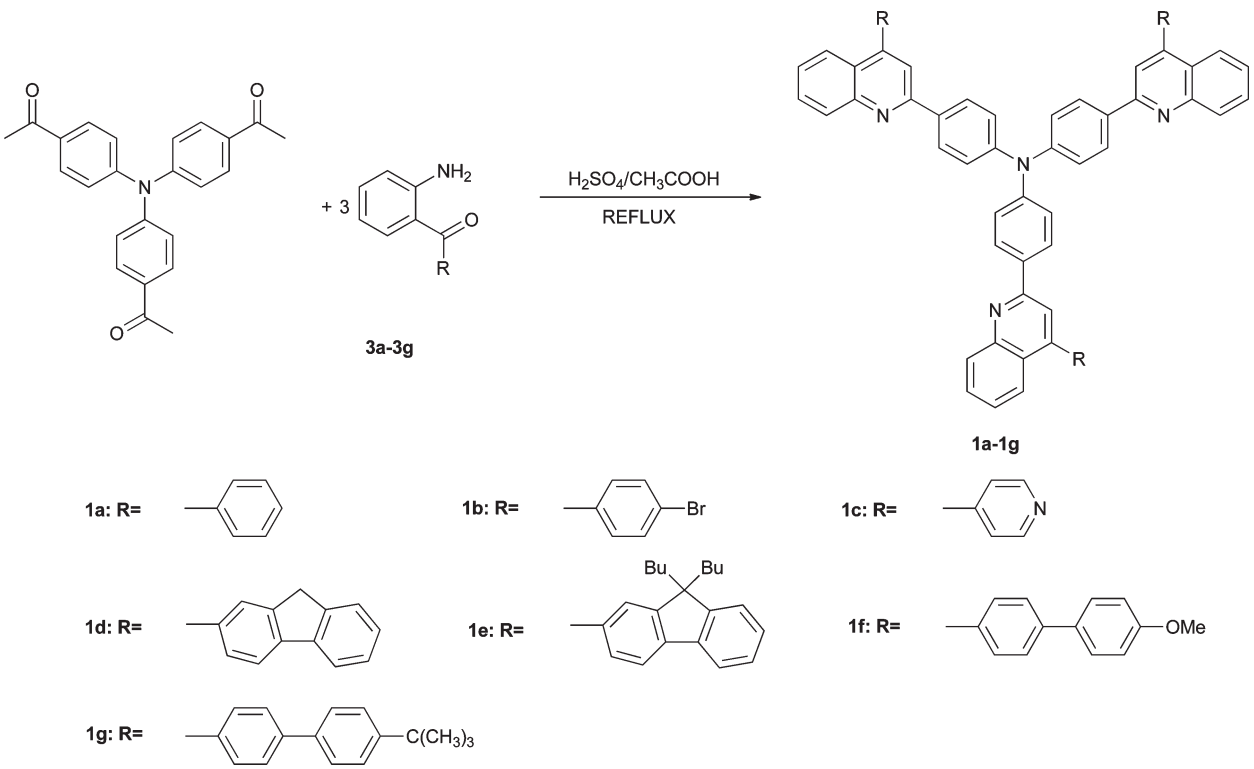

Scheme 1 Synthesis of starburst multifunctional molecules **1a–1g** by a Friedländer reaction.

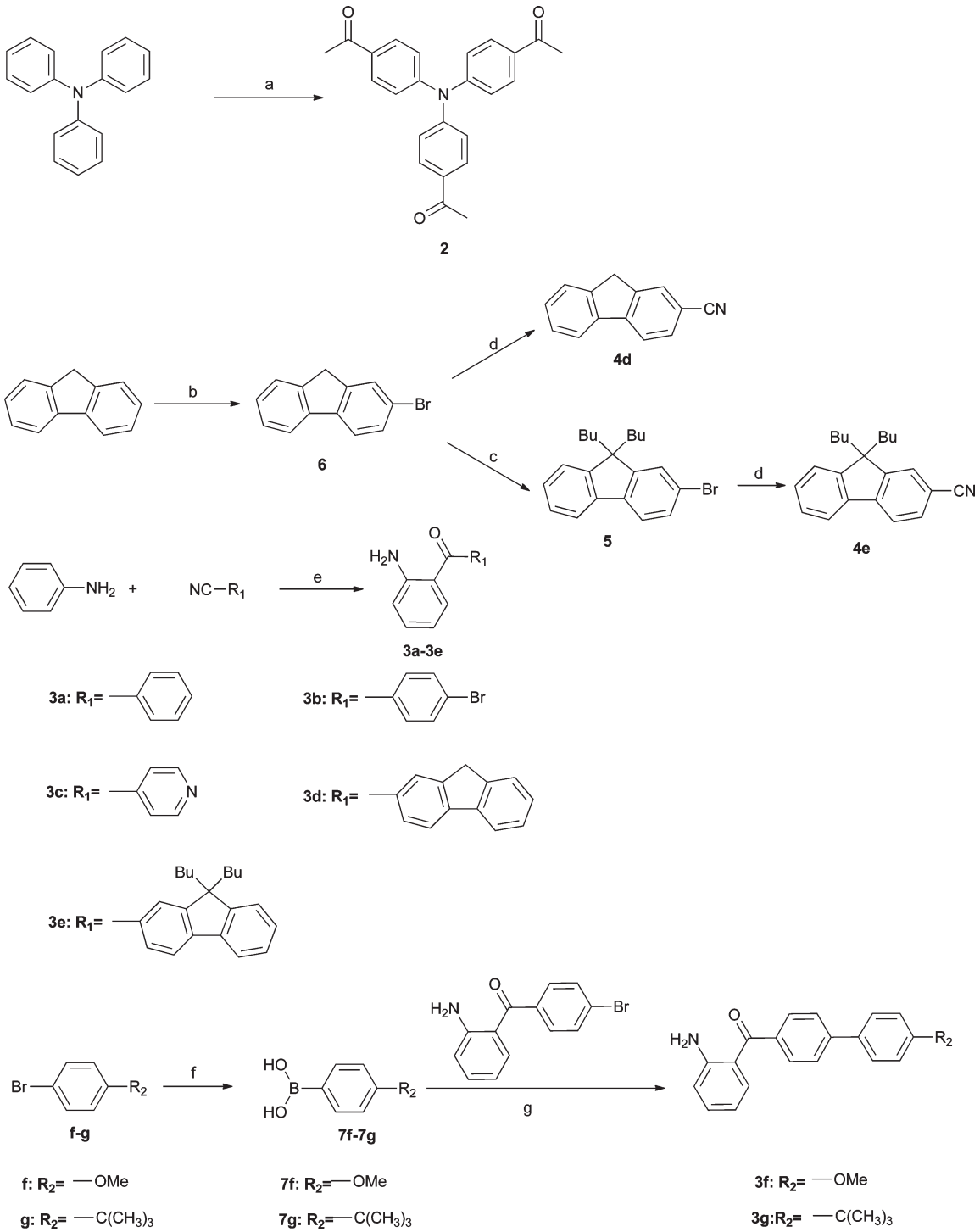

Scheme 2 Reagents and conditions: (a) acetyl chloride, $AlCl_3$, DCM, reflux; (b) NBS, propylene carbonate, 60 °C;[47] (c) *n*-butyl bromide, KOH, KI, DMSO, 60 °C;[48] (d) CuCN, NMP, reflux;[49] (e) (i) BCl_3, 1,1,2,2-tetrachloroethane, reflux; (ii) HCl–H_2O, 80 °C; (f) (i) Mg, THF, reflux; (ii) $B(OCH_3)_3$, −78 °C;[50,51] (iii) HCl–H_2O; (g) $Pd(AcO)_2$, K_2CO_3, DMF + H_2O, 80 °C.

presence of stoichiometric amounts of BCl_3 in 54.6%–35.3% yield, respectively.[31] The decrease in the yield might be due to the increase in the conjugate structure. The other intermediates **3f** and **3g** were obtained by the palladium-catalyzed Suzuki cross-coupling with compound **3b** and compound **7f** or **7g**, respectively (Scheme 2) in the desired yield of 80.5% and 79.3%.[32] The synthetic routes to other intermediates are outlined in Scheme 2. ^1H NMR spectra, ^{13}C NMR spectra, elemental analysis and FTIR spectra on **1a–1g** confirmed the proposed structures.

Thermal properties

The thermal properties, including glass transition and decomposition temperatures, of these molecules (**1a–1g**) are shown in

Table 1 Photophysical properties of starbursts **1a–1g**

	λ_{max}^{Abs} (nm)		λ_{max}^{Em} (nm)			E_g^{opt} (eV)		Stokes shift (nm)		
Compound	Toluene	Solid-state	Toluene	Solid-state	Φ_u	Toluene	Solid-state	Toluene	Solid-state	T_g/T_d
1a	295(3.46[a]) 400(6.232)	405	433	482	0.71	2.35	1.67	33	77	229.8/>500
1b	297(9.11) 401(15.97)	388	439	483	0.98	2.33	1.65	38	95	205.3/>500
1c	299(3.82) 403(7.34)	407	446	486	0.61	2.31	1.64	43	79	301.9/>500
1d	309(8.52) 400(9.04)	397	437	483	0.58	2.34	1.65	38	86	366.7/>500
1e	313(7.18) 401(7.61)	425	437	461	0.61	2.33	1.65	36	36	176/405.9
1f	296(9.62) 400(10.45)	410	438	502	0.57	2.34	1.66	38	92	298.7/>500
1g	294(7.21) 401(8.01)	413	437	486	0.58	2.32	1.65	36	73	248.8/>500

[a] The values in brackets are molar extinction coefficient, 10^4 M^{-1} cm^{-1}.

Table 1. Differential scanning calorimetry (DSC) was used to investigate phase transitions (**1a** and **1b** are shown in Fig. 1, the others are shown in Table S1 in ESI†). All the seven compounds (**1a–1g**) exhibit very high glass transition temperatures (T_g) ranging from 176.4 °C for 9,9-*n*-dibutyl-fluorenyl substituted **1e** to 366.7 °C for fluorenyl substituted **1d**. **1a–1g** are thermally stable up to 400 °C as shown by their high decomposition temperatures (T_d) in the thermogravimetric analysis (TGA) measurements. The T_g of **1a–1g** is much higher than that of the commonly used hole-transporting material (*e.g.*, 98 °C for NPB) and previously reported TQTPA (T_g = 130 °C).[26,33] Therefore, all of these results demonstrate that the series of triphenylamine-centered starburst quinolines **1a–1g** are very robust molecules.

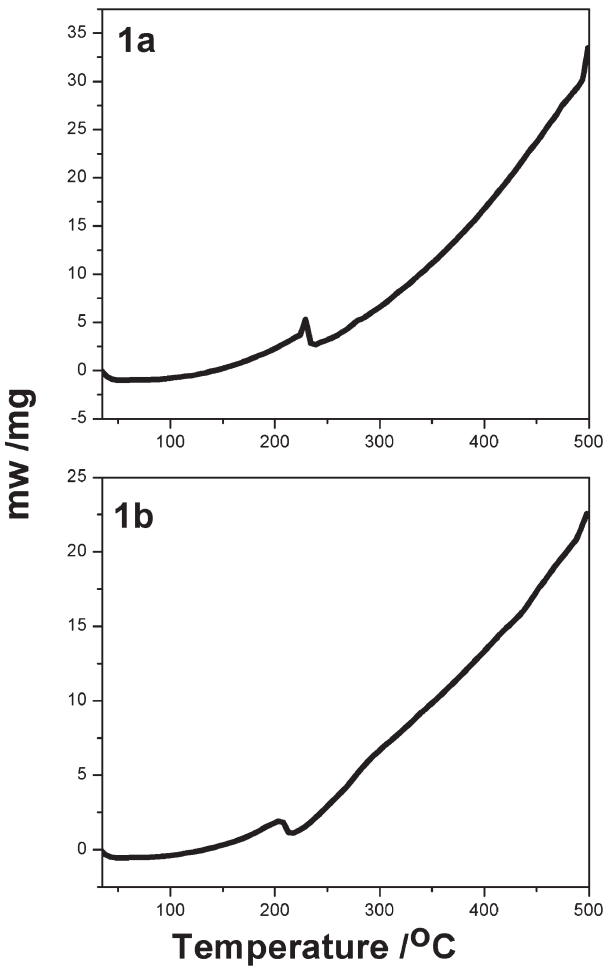

Fig. 1 DSC thermograms of **1a** and **1b** under a nitrogen atmosphere at a heating rate of 10 °C min^{-1}.

Photophysical properties

Comparisons of **1a–1g** in visible light and UV light in toluene solution are shown in Fig. 2. The solution of **1a–1g** appears as light blue fluorescence in visible light and emits blue fluorescence in UV light (band 254 nm).

The absorption and photoluminescence spectra of **1a–1g** were investigated both in solutions and in solid-states. Fig. 3 shows the absorption spectra of **1a–1g** in toluene solution. The solution absorption spectra of **1a–1g** show two bands, a lower intensity band in the 260 to 320 nm range and a higher intensity band in the 390 to 430 nm range. With the exception of the starbursts with fluorenyl and 9,9-dibutyl-fluorenyl substituents, **1d** and **1e**, all the others have very similar absorption spectra with two peaks in the range of 294 to 299 nm and 400 to 403 nm. Both peaks have large molar extinction coefficients (ε), shown in Table 1. These absorption bands in the spectra of **1a–1g** are associated with π–π* transitions. As expected, the absorption peaks are red-shifted to 309 nm, 400 nm in **1d** and 313 nm, 401 nm in **1e** owing to the increase in conjugation length with fluorenyl and 9,9-dibutyl-fluorenyl substitution.

The absorption spectra of **1a–1g** in the solid-state are shown in Fig. 3. In addition to their broad featureless characteristics, these solid-state absorption bands are significantly red-shifted from the dilute solution spectra for **1a**, **1c**, **1e**, **1f**, **1g**. The 4–24 nm red shifts in the absorption maximum for **1a**, **1c**, **1e**, **1f** and **1g** suggest there is a slight increase in conjugation length in

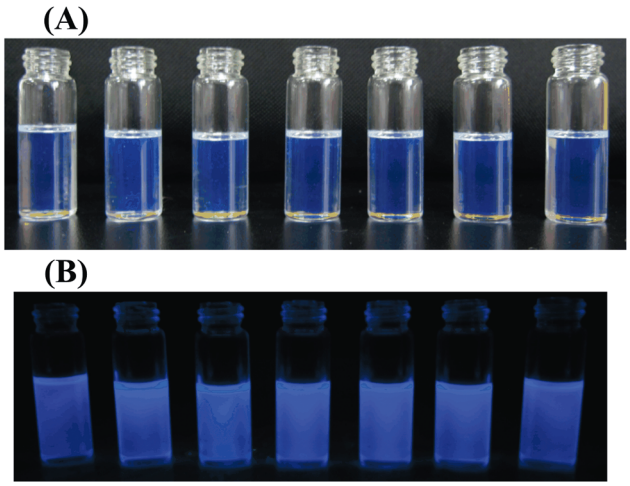

Fig. 2 (a) Color comparison of **1a–1g** in visible light in toluene (10^{-5} M); (b) color comparison of **1a–1g** in UV in toluene (10^{-5} M).

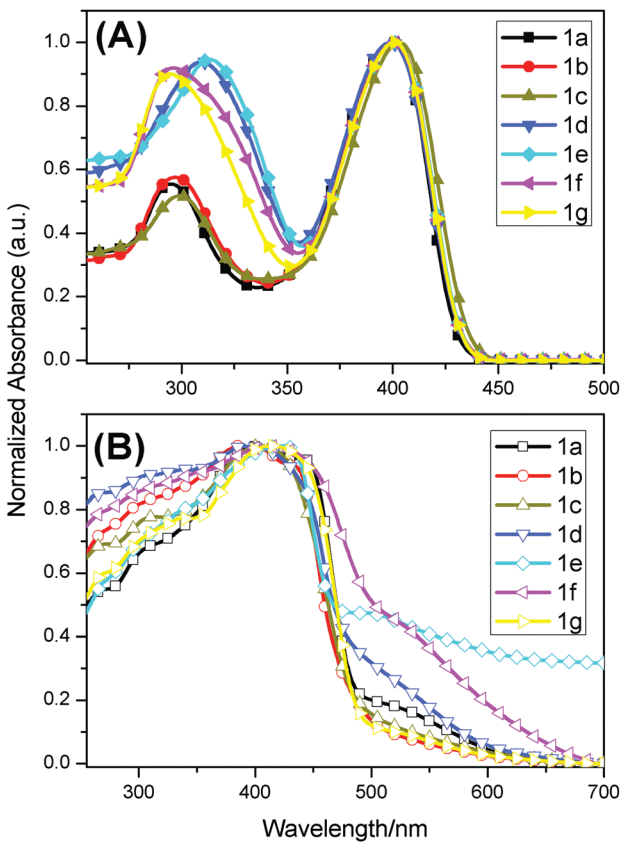

Fig. 3 (a) UV–vis absorption spectra of **1a–1g** in toluene solution (10^{-5} M); (b) UV–vis absorption spectra of **1a–1g** in solid-state.

the solid-state. Such an increase in conjugation length in the solid-state is expected from the more planar conformations due to the π-stacking in the solid-state. Optical band gaps (E_g^{opt}) determined from the absorption edge of the solution and solid-state spectra are given in Table 1. The optical band gap varies from 2.31 to 2.35 eV for the solution and from 1.64 to 1.67 eV for the solid-state.

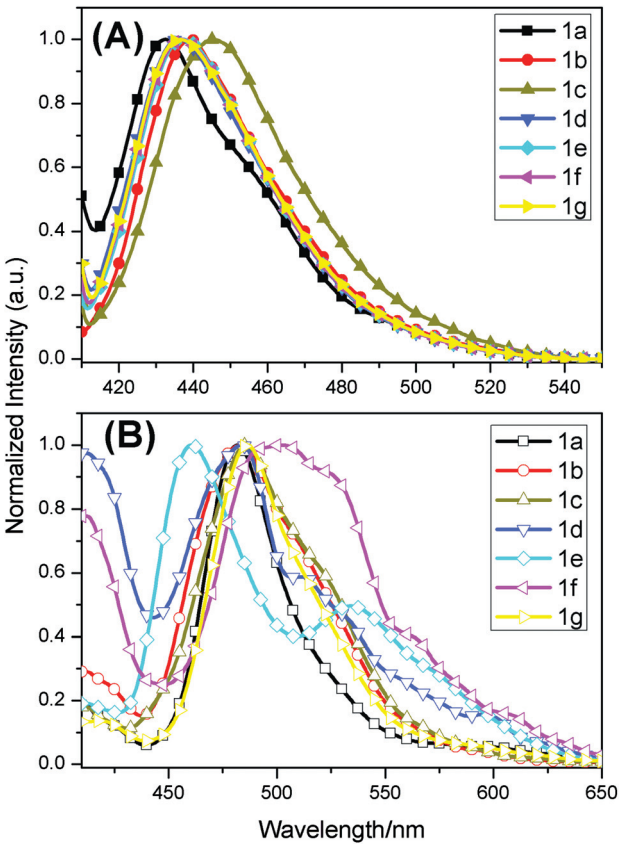

Fig. 4 (a) Photoluminescence spectra of **1a–1g** in toluene solution (10^{-8} M); (b) photoluminescence spectra of **1a–1g** in solid-state.

All seven molecules **1a–1g** emit blue light with the emission maximum ranging from 433 nm for **1a** to 446 nm for **1c** with a narrow full-width-at-half-maximum (FWHM) of 40–45 nm (Fig. 4). All the λ_{max}^{Em} of **1b–1g** are slightly red shifted compared to **1a**. Similarly pyridyl substituted **1c** has the maximum red shift (13 nm). The Stokes shift is small for all the compounds, ranging from 33 to 43 nm. Using quinine sulfate (Φ_s = 0.546 in 0.1 N H_2SO_4)[34–36] as a reference, the fluorescence quantum yields (Φ_u) of **1a–1g** in toluene have been shown in Table 1. The Φ_u of compounds **1a–1g** in dilute solution in toluene was relatively high, ranging from 0.57 for **1f** to 0.98 for **1b** (Table 1). **1c–1g** have almost identical values of 0.57–0.61, whereas **1a** and **1b** have the highest PL quantum yields at 0.71 and 0.98. The decrease in the quantum yield may be due to the increase in the conjugate structure.

The blue emission observed in solution is retained in the solid-state with PL emission maxima in the range of 461 nm for **1e** to 502 nm for **1f** (Fig. 4). Compared to the solutions, the maximum emission peaks of the solid state have a red-shift of 23 nm to 64 nm. The similarities of the emission spectral features in conjunction with the π-stacking of the molecules in the solid-state suggest that excimer emission[37,38] best describes the solid-sate luminescence of **1a–1g**. The solid-state PL emission spectra are also much broader compared to the solution spectra, with a FWHM ranging from 44 nm to 80 nm. In contrast, **1c** has a broad PL spectrum with a shoulder peak at 502 nm and a FWHM of 80 nm. The broad PL emission spectrum of **1c**

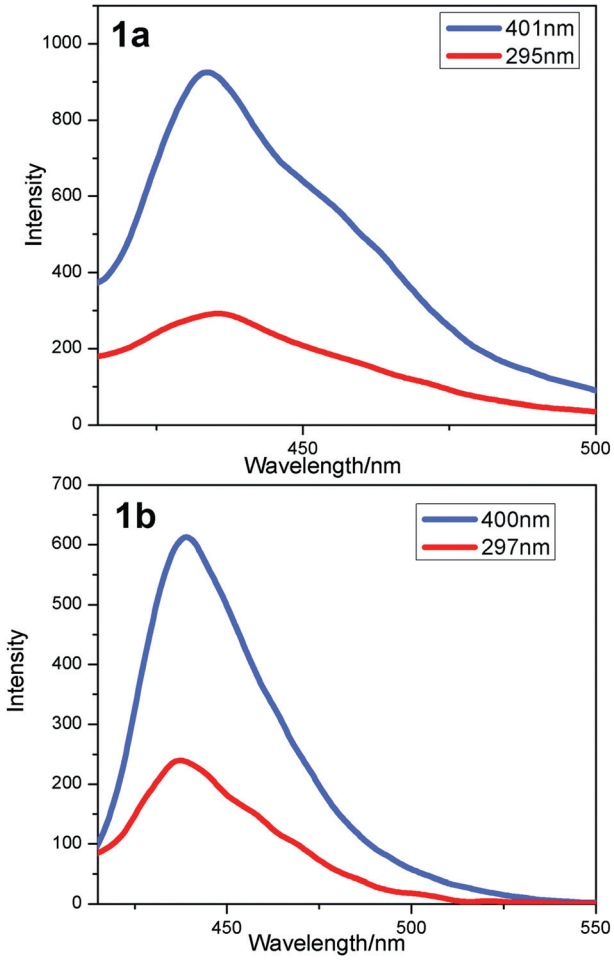

Fig. 5 Fluorescence spectra of **1a** and **1b** in toluene solutions at different excitation wavelengths.

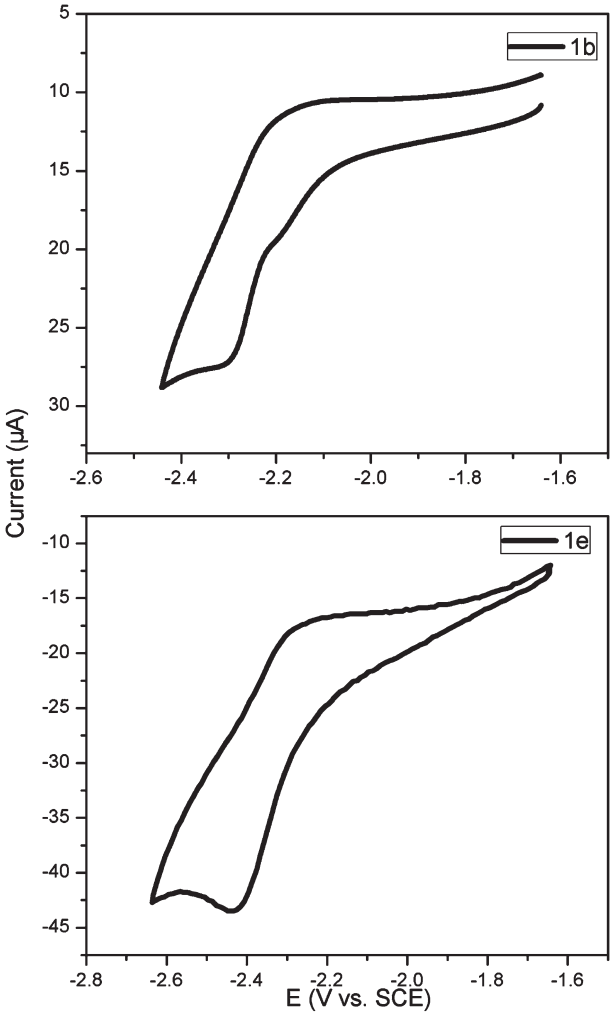

Fig. 6 The reduction cyclic voltammograms of **1b** and **1e** in solution.

suggests that it favors strong aggregation compared to the other compounds.

When the starbursts are excited in the absorption range of 290–320 nm or 390–410 nm, the emission spectra for all seven molecules **1a–1g** only show one emission peak from the core. The single emission upon excitation of quinoline arms suggests the occurrence of efficient intramolecular energy transfer[39,40] (**1a** and **1b** are shown in Fig. 5, the others are shown in Table S2 in the ESI†).

Electrochemical properties

The reduction cyclic voltammograms (CVs) of **1b** and **1e** in solution are shown in Fig. 6 while the reduction CVs of **1a**, **1c**, **1d**, **1f**, **1g** are shown in the ESI (Table S3†). Irreversible reduction peaks were seen in the CVs of **1a–1b** and **1d–1g**, whereas quasireversible reduction peaks were seen in the CVs of **1c**. A formal reduction potential varies from −2.18 V for **1c** to −2.44 V for **1e** (*vs.* SCE) and the onset reduction potentials of **1a–1g** are in the range of −2.05 to −2.24 V (*vs.* SCE). Table 2 shows the solution electrochemical data for **1a–1g**. Electron affinities (EA) were estimated from the onset of the reduction waves in the solution CVs (EA = E_{red}^{onset} + 4.4 eV) by using an SCE energy level of 4.4 eV *versus* vacuum.[41–43] These compounds had EA values of 2.16–2.35 eV (below vacuum). The reduction potentials of all the molecules are relatively unchanged by the substituent (R groups), indicating that the effect of the substituent is weak.

Molecules **1a**, **1b**, **1d**, **1e**, **1g** had one irreversible oxidation peak. In the case of **1c** and **1f**, the irreversible oxidation peak was not seen (**1b** and **1e** in solution are shown in Fig. 7, while the oxidation CVs of **1a**, **1d**, **1g** are shown in Table S3 in the ESI†). The five molecules **1a**, **1b**, **1d**, **1e**, **1g** display very similar CVs with a formal potential of 1.52–2.18 V (*vs.* SCE) and E_{ox}^{onset} in the range of 1.46–2.05 V (*vs.* SCE). Ionization potentials (IP) of **1c** and **1f** were estimated using the optical bandgap determined from optical absorption edge (Table 1): IP = EA + E_g^{opt} [44] and **1a**, **1b**, **1d**, **1e**, **1g** were estimated using the E_{ox}^{onset} (Table 2): IP = E_{ox}^{onset} + 4.4 eV. [41–43] As a result the IP is reduced from 4.54 eV in **1f** to 6.45 eV in **1a**. The estimated IP show rather deep HOMO energy levels for this class of electron transport materials. These IP values are significantly near or higher than those of well-known electron transport materials (ETMs), including tris(8-hydroxyquinoline)aluminium (Alq_3) (IP = 5.7–5.9 eV),[45] and previously reported oligoquinolines

Table 2 Electrochemical properties of solution and energy values theoretically calculated for molecules of **1a–1g** in the gas phase

Compound	E_{red}^{peak} (V)	E_{red}^{onset} (V)	EA (eV)	E_{ox}^{peak} (V)	E_{ox}^{onset} (V)	IP (eV)	HOMO (eV)	LUMO (eV)	E_g^{cal} (eV)
1a	−2.29	−2.14	2.26	2.18	2.05	6.45	−4.86	−1.29	3.57
1b	−2.29	−2.16	2.24	2.12	2.02	6.42	−4.99	−1.47	3.52
1c	−2.18	−2.05	2.35	—	—	4.66	−5.05	−1.57	3.48
1d	−2.43	−2.20	2.20	1.52	1.46	5.86	−4.84	−1.32	3.52
1e	−2.44	−2.24	2.16	1.57	1.50	5.90	−4.84	−1.33	3.51
1f	−2.30	−2.20	2.20	—	—	4.54	−4.81	−1.27	3.54
1g	−2.30	−2.18	2.22	1.67	1.58	5.98	−4.84	−1.31	3.53

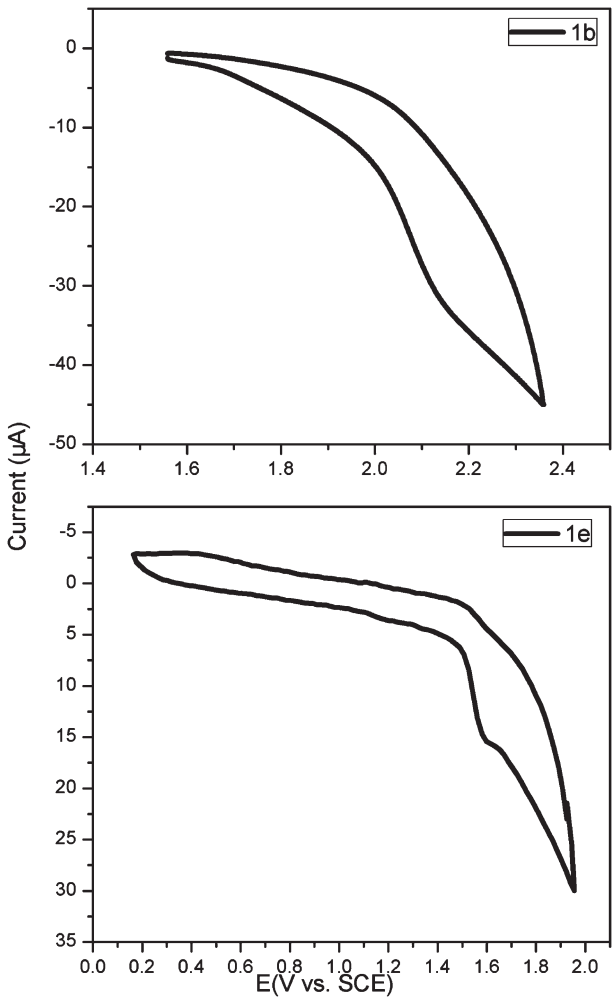

Fig. 7 The oxidation cyclic voltammograms of **1b** and **1e** in solution.

(IP = 5.53–5.81 eV).[43] This suggests that the seven triphenylamine-centered starburst quinolines (**1a–1g**) can be used as wide-energy gap ETMs and they could also be used for an excellent hole-blocking layer in OLEDs.

Theoretical calculations

The geometry and the HOMO and LUMO energy levels of **1a–1g** were optimized using density functional theory (DFT) method at the B3LYP/6-31G* level, as implemented in Gaussian 09 program.[46] The core triphenylamine (TPA) group in these molecules shows the three-dimensional propeller structure, quinoline groups are nearly coplanar with triphenylamine group and the substituents on the quinoline unit (R group) are twisted from the plane of the quinoline unit. This geometry could result in good solution processability which was confirmed with experimental results that show **1a–1g** were soluble in most solvents like chloroform, tetrahydrofuran, toluene and so on. The HOMO of **1a–1g** is located on the TPA unit, whereas the LUMO is located predominantly on the two arms of the molecule (see Table S4 in the ESI†). The broad distribution of the HOMO should be good for the hole transport through the molecules when **1a–1g** are used as hole-injecting/hole-transporting materials in OLEDs. **1a–1g** have the HOMO (−5.05 to −4.81 eV, shown in Table 2) close to the work function of ITO and thus allow efficient hole injection from the ITO. Therefore **1a–1g** were expected to have hole-injecting/hole-transport capacity. The LUMO is shown in Table 2. The LUMO energy values of **1a–1g** were from −1.27 to −1.57 eV, respectively. The HOMO–LUMO energy differences (energy band gaps, calculated E_g^{cal}) at B3LYP/DFT level of theory are presented in Table 2. The result indicates that E_g^{cal} values decrease as the length of π-conjugated system increases. These predicted E_g^{cal} values are much higher than those estimated from the onset of UV–vis absorption (E_g^{opt}). There are factors which may be responsible for the errors because the orbital energy difference between HOMO and LUMO is still an approximate estimation to the transition energy since the transition energy also contains significant contributions from some two-electron integrals. The real situation is that an accurate description of the lowest singlet excited state requires a linear combination of a number of excited configurations.

Conclusions

We have synthesized seven triphenylamine-centered starburst quinolines **1a–1g**, and characterized them with ^{1}H and ^{13}C NMR spectroscopy, elemental analysis and IR. The new triphenylamine-centered starburst quinolines combined relatively high fluorescence quantum yields (0.98 to 0.57) with high ionization potentials (4.54 to 6.45 eV), high glass transition temperatures (above 176.4 °C) and high decomposition temperatures (above 406 °C). These compounds also have the HOMO (−5.05 to −4.81 eV, respectively) close to the work function of ITO. These results demonstrate that the triphenylamine-centered starburst quinolines **1a–1g** are very promising hole-transporting, blue emitting, electron-transport materials and the host-materials of a dopant for hole-injecting for applications for developing high-efficiency OLEDs with a simple architecture. Furthermore, we

will investigate the preparation of devices from solution processing and their electroluminescence and improve device performance with these starbursts as hole-injecting/hole-transporting/light-emitting/electron-transport layera.

Notes and references

1 C. W. Tang and S. A. VanSlyke, *Appl. Phys. Lett.*, 1987, **51**, 913–915.
2 J. Kido, M. Kimura and K. Kagai, *Science*, 1995, **267**, 1332.
3 R. H. Friend, R. W. Gymer, A. B. Holmes, J. H. Burroughes, R. N. Marks, C. Taliani, D. D. C. Bradley, D. A. Dos Santos, J. L. Bredas, M. Logdlund and W. R. Salaneck, *Nature (London)*, 1999, **397**, 121–128.
4 M. A. Baldo, M. E. Thompson and S. R. Forrest, *Nature (London)*, 2000, **403**, 750–753.
5 L. S. Hung and C. H. Chen, *Mater. Sci. Eng., R: Reports*, 2002, **39**, 143–222.
6 R. F. Service, *Science (Washington, DC, U. S.)*, 2005, **310**, 1762–1763.
7 F. So, J. Kido and P. Burrows, *MRS Bull.*, 2008, **33**, 663–669.
8 S. Reineke, F. Lindner, G. Schwartz, N. Seidler, K. Walzer, B. Luessem and K. Leo, *Nature (London, U. K.)*, 2009, **459**, 234–238.
9 B. W. D'Andrade and S. R. Forrest, *Adv. Mater.*, 2004, **16**, 1585–1595.
10 H. Aziz, Z. D. Popovic, N.-X. Hu, A.-M. Hor and G. Xu, *Science (Washington, D. C.)*, 1999, **283**, 1900–1902.
11 C. W. Tang, S. A. VanSlyke and C. H. Chen, *J. Appl. Phys.*, 1989, **65**, 3610–3616.
12 A. W. Freeman, S. C. Koene, P. R. L. Malenfant, M. E. Thompson and J. M. J. Fréchet, *J. Am. Chem. Soc.*, 2000, **122**, 12385–12386.
13 Y. Shirota, *J. Mater. Chem.*, 2000, **10**, 1–25.
14 P. Furuta, J. Brooks, M. E. Thompson and J. M. J. Fréchet, *J. Am. Chem. Soc.*, 2003, **125**, 13165–13172.
15 T. D. Anthopoulos, M. J. Frampton, E. B. Namdas, P. L. Burn and I. D. W. Samuel, *Adv. Mater.*, 2004, **16**, 557–560.
16 T. W. Kwon, M. M. Alam and S. A. Jenekhe, *Chem. Mater.*, 2004, **16**, 4657–4666.
17 E. Holder, B. M. W. Langeveld and U. S. Schubert, *Adv. Mater.*, 2005, **17**, 1109–1121.
18 Z. H. Li, M. S. Wong, H. Fukutani and Y. Tao, *Org. Lett.*, 2006, **8**, 4271–4274.
19 P. L. Burn, S. C. Lo and I. D. W. Samuel, *Adv. Mater.*, 2007, **19**, 1675–1688.
20 D. H. Choi, K. I. Han, I.-H. Chang, S.-H. Choi, X.-H. Zhang, K.-H. Ahn, Y. K. Lee and J. Jang, *Synth. Met.*, 2007, **157**, 332–335.
21 H. J. Bolink, E. Barea, R. D. Costa, E. Coronado, S. Sudhakar, C. Zhen and A. Sellinger, *Org. Electron.*, 2008, **9**, 155–163.
22 Z. Zhao, Z. Li, J. W. Y. Lam, J.-L. Maldonado, G. Ramos-Ortiz, Y. Liu, W. Yuan, J. Xu, Q. Miao and B. Z. Tang, *Chem. Commun.*, 2011, **47**, 6924–6926.
23 Y. Shirota and H. Kageyama, *Chem. Rev.*, 2007, **107**, 953–1010.
24 Z. Ning and H. Tian, *Chem. Commun.*, 2009, 5483–5495.
25 C. J. Tonzola, M. M. Alam, W. Kaminsky and S. A. Jenekhe, *J. Am. Chem. Soc.*, 2003, **125**, 13548–13558.
26 S. Tao, L. Li, J. Yu, Y. Jiang, Y. Zhou, C.-S. Lee, S.-T. Lee, X. Zhang and O. Kwon, *Chem. Mater.*, 2009, **21**, 1284–1287.
27 Jilin University, , *CN Pat.*, 101423757A, 2009.
28 Mitsubishi Chemical Corporation, , *JP Pat.*, 2002175883A, 2002.
29 J. A. Mikroyannidis, M. Fakis and I. K. Spiliopoulos, *J. Polym. Sci., Part A: Polym. Chem.*, 2009, **47**, 3370–3379.
30 Y.-Q. Xu, J.-M. Lu, N.-J. Li, F. Yan, X.-W. Xia and Q.-F. Xu, *Eur. Polym. J.*, 2008, **44**, 2404–2411.
31 T. Sugasawa, T. Toyoda, M. Adachi and K. Sasakura, *J. Am. Chem. Soc.*, 1978, **100**, 4842–4852.
32 L. Liu, Y. Zhang and B. Xin, *J. Org. Chem.*, 2006, **71**, 3994–3997.
33 L. S. Hung and C. H. Chen, *Mater. Sci. Eng., R: Reports*, 2002, **39**, 143–222.
34 W. R. Dawson and M. W. Windsor, *J. Phys. Chem.*, 1968, **72**, 3251–3260.
35 G. A. Crosby and J. N. Demas, *J. Phys. Chem.*, 1971, **75**, 991–1024.
36 D. F. Eaton, *Pure Appl. Chem.*, 1988, **60**, 1107–1114.
37 S. A. Jenekhe and J. A. Osaheni, *Science*, 1994, **265**, 765–768.
38 J. A. Osaheni and S. A. Jenekhe, *Macromolecules*, 1994, **27**, 739–742.
39 M. G. Ren, H. J. Guo, F. Qi and Q. H. Song, *Org. Biomol. Chem.*, 2011, **9**, 6913–6916.
40 Z. F. a. L. J. Song Xinqi, *Photochemistry Principles Techniques Applications*, Higher Education Press, Bei Jing, 2001.
41 A. K. Agrawal and S. A. Jenekhe, *Chem. Mater.*, 1996, **8**, 579–589.
42 S. Liu, Q. Wang, P. Jiang, R. Liu, G. Song, H. Zhu and S.-W. Yang, *Dyes Pigm.*, 2010, **85**, 51–56.
43 Q. Zhang, P. Jiang, K. Wang, G. Song and H. Zhu, *Dyes Pigm.*, 2011, **91**, 89–97.
44 C. J. Tonzola, A. P. Kulkarni, A. P. Gifford, W. Kaminsky and S. A. Jenekhe, *Adv. Funct. Mater.*, 2007, **17**, 863–874.
45 A. Rajagopal and A. Kahn, *Adv. Mater.*, 1998, **10**, 140–144.
46 G. W. T. M. J. Frisch, H. B. Schlegel, G. E. Scuseria, M. A. Robb, J. R. Cheeseman, G. Scalmani, V. Barone, B. Mennucci, G. A. Petersson, H. Nakatsuji, M. Caricato, X. Li, H. P. Hratchian, A. F. Izmaylov, J. Bloino, G. Zheng, J. L. Sonnenberg, M. Hada, M. Ehara, K. Toyota, R. Fukuda, J. Hasegawa, M. Ishida, T. Nakajima, Y. Honda, O. Kitao, H. Nakai, T. Vreven, J. A. Montgomery, Jr., J. E. Peralta, F. Ogliaro, M. Bearpark, J. J. Heyd, E. Brothers, K. N. Kudin, V. N. Staroverov, R. Kobayashi, J. Normand, K. Raghavachari, A. Rendell, J. C. Burant, S. S. Iyengar, J. Tomasi, M. Cossi, N. Rega, J. M. Millam, M. Klene, J. E. Knox, J. B. Cross, V. Bakken, C. Adamo, J. Jaramillo, R. Gomperts, R. E. Stratmann, O. Yazyev, A. J. Austin, R. Cammi, C. Pomelli, J. W. Ochterski, R. L. Martin, K. Morokuma, V. G. Zakrzewski, G. A. Voth, P. Salvador, J. J. Dannenberg, S. Dapprich, A. D. Daniels, Ö. Farkas, J. B. Foresman, J. V. Ortiz, J. Cioslowski and D. J. Fox, Gaussian Inc., Wallingford CT, 2009.
47 R. Kannan, G. S. He, T.-C. Lin, P. N. Prasad, R. A. Vaia and L.-S. Tan, *Chem. Mater.*, 2004, **16**, 185–194.
48 C.-C. Chang, H. Yueh and C.-T. Chen, *Org. Lett.*, 2011, **13**, 2702–2705.
49 K. A. Nguyen, J. E. Rogers, J. E. Slagle, P. N. Day, R. Kannan, L.-S. Tan, P. A. Fleitz and R. Pachter, *J. Phys. Chem. A*, 2006, **110**, 13172–13182.
50 S. Bruns, V. Sinnwell and J. Voss, *Magn. Reson. Chem.*, 2003, **41**, 269–272.
51 W. Y. Huang and S. Y. Huang, *Macromolecules*, 2010, **43**, 10355–10365.